

Spin-down of neutron stars by neutrino emission

Maxim Dvornikov^{a,b*} and Claudio Dib^{a†}

^a*Centro Científico-Tecnológico de Valparaíso and Departamento de Física,
Universidad Técnica Federico Santa María, Casilla 110-V, Valparaíso, Chile;*

^b*IZMIRAN, 142190, Troitsk, Moscow Region, Russia*

(Dated: November 1, 2018)

We study the spin-down of a neutron star during its early stages due to the neutrino emission. The mechanism we consider is the subsequent collisions of the produced neutrinos with the outer shells of the star. We find that this mechanism can indeed slow down the star rotation but only in the first tens of seconds of the core formation, which is when the appropriate conditions of flux and collision rate are met. We find that this mechanism can extract less than 1% of the star angular momentum, a result which is much less than previously estimated by other authors.

PACS numbers: 97.60.Bw, 14.60.Lm, 26.60.Gj

Keywords: supernova neutrinos; rotating neutron stars

I. INTRODUCTION

Neutrinos play a significant role in the evolution of various astronomical objects. They should carry away almost all of the gravitational energy lost in the collapse of a massive star during a supernova explosion [1], phenomenon that was confirmed by the detection of neutrinos from supernova SN1987A, in the available experiments at the time, namely Kamiokande-II [2], IMB [3], Baksan [4], and LSD [5]. Neutrinos are also important in the cooling of the neutron star formed at the center of a supernova explosion [6, 7]. Neutrinos, because of their weak interaction with matter, provide important signals of the inner parts of stars like our Sun [8] and of the cores in stellar collapses [9]. Asymmetric neutrino emission may also be responsible for the large peculiar velocities observed in pulsars [10, 11]. It has also been proposed a long time ago that neutrino emission can slow down the spinning of neutron stars [12, 13]. Here we want to revisit the latter idea, trying to refine the estimate by using our current knowledge of the physics of neutrinos and their emission in neutron stars.

The majority of neutron stars are known to have large angular velocities, and in the case of radio pulsars one can directly measure their speed of rotation. It is also observed that, on average, their rotation tends to slow down with time, a phenomenon that is explained by emission of electromagnetic waves or, in some conditions, by the emission of gravitational waves or other processes [14]. This should be the case during most of the life of the neutron star. However, at the early stages, during the collapse and formation of the star core (in a time scale of 10s), which is when the flux is intense enough and the mean free path is comparable to the star size [15], the spin-down of this protoneutron star (PNS) can be influenced by the collisions of the neutrinos with the star matter as they escape. It is interesting to notice that

the opposite effect, i.e. the acceleration of a neutron star rotation, has also been proposed [16] for the case of neutrinos interacting with strong toroidal magnetic fields inside stars.

Note that neutrino emission can also decrease the angular momentum of the star due to the change in the gravitational mass of the star [17–19]. According to the estimate of Ref. [19], a star can lose at most 40% of its initial angular momentum. Other proposed mechanisms of angular momentum loss at early stages of the PNS evolution include viscous processes [20], transfer of rotational energy into the energy of the supernova explosion [21], magnetic PNS winds [22], and propeller mechanisms [23]. However, it was found in Ref. [24] that none of these theoretical explanations can robustly spin-down a PNS from about several ms to the observed periods of rotation of young pulsars. We must add that the loss of angular momentum by neutrino emission may also occur if there is anisotropy at the neutrino production points, which may be the case if the star matter has significant polarization due to the star magnetic field [25]. However, we do not consider this effect here. In our work we are interested in the case in which the production is rather isotropic, but neutrinos travel a sizable distance in the star and subsequently scatter with matter in outer shells where the transverse velocity of the medium is larger.

In this work we revise the previous estimates for the spin-down of PNS by neutrino emission [12, 13], where it was stated that this mechanism can even possibly stop the star rotation. This result denotes a very dramatic effect, which we want to study using a more detailed work, but still within analytical models in order to study the sensitivity of our results to different parameters of a generic star. Our estimates show that the effect is much weaker than previous estimates – less than 1% reduction of the angular speed. We also check that most refinements in our treatment point to further reduction, not enhancement, of the effect.

In Sec. II we present our conceptual treatment and calculation of the spin-down of PNS due to neutrino emission. In Sec. III we summarize our results and state our

* maxim.dvornikov@usm.cl

† claudio.dib@usm.cl

conclusions.

II. MODEL AND CALCULATIONS

In this section we formulate the phenomenon of spin-down of a forming neutron star due to neutrino emission during the core collapse. The spin-down mechanism consists in the fact that neutrinos which escape from the star are produced in regions around the neutrinosphere, where the transverse velocity of matter is relatively lower, and as they propagate to outer regions, some of them will collide with matter moving with larger transverse velocities, thus absorbing transverse momentum and causing a spin down of the medium. In this sense, the trajectory of an outgoing neutrino should bend as it propagates through the rotating medium, due to collisions. For this effect to be of any significance, the mean free path should be less (but not much less) than the star radius. Otherwise, if the mean free path is much larger, there will be too few collisions, while if it is much shorter, the difference in transverse velocities from the emission to the collision points will be too small.

As cited above, spin-down due to neutrino emission was already proposed in the past. However, with the knowledge available today we can include more details in the treatment, namely (i) take proper account of the weak interactions in the collisions, (ii) use a phenomenological matter composition and density profile in the star instead of a uniform medium, (iii) take into account the opacity of inner parts of the star where neutrinos thermalize, so for the spin-down effect neutrinos are emitted only from a *neutrinosphere* instead of from the center of the star, and (iv) use thermal spectra for each neutrino species instead of a single monochromatic emission.

We organize the calculation starting from the neutrino production at the neutrinosphere, followed by the individual neutrino collisions with the rotating medium further outside, and finally, by adding these collisions all around the star, to get the result. At each step we state the model of the situation and the approximations used.

Neutrinos are produced everywhere around the star, but at high temperatures (energies) they suffer much scattering and absorption. Therefore, those which manage to escape are not produced at the star center but at the neutrinosphere, or surface of last scattering [26]. The definition of the neutrinosphere is statistical and depends on the medium density as well as the neutrino species and energy. Here we will simply define it as a spherical shell of radius R_{ns} , different for every neutrino species and energy, given by one mean free path less than the star radius,

$$R_{ns} = R - \frac{1}{\sigma_\nu n}, \quad (2.1)$$

where R is the star radius and σ_ν is the (energy-dependent) total cross section for neutrino scattering in the star medium with nucleon number density n . Since

n depends on the position, Eq. (2.1) is really an equation for R_{ns} that we solve in each case. We consider a PNS medium where a fraction $Y_n \sim 0.9$ of the nucleons are neutrons and a fraction $Y_p \sim 0.1$ are protons [6].

We neglect scattering with electrons, because they are in equal number to protons but their cross section is an order of magnitude smaller. We also neglect Pauli blocking or nucleon correlations. These effects should be more important at later stages of the star evolution, when neutrino energies are lower; however, the spin-down caused by neutrinos is negligible then. In any case, correlations tend to reduce the cross sections [27], pointing further into the direction that previous calculations of the PNS spin-down by neutrinos were overestimated.

The total cross sections (and thus neutrinospheres) differ for three species of neutrinos: electron neutrinos ν_e , electron antineutrinos $\bar{\nu}_e$, and all other ν_x . The neutrino-nucleon cross sections, for neutrinos with energies 1–100 MeV, are approximately (see pp. 160–167 in Ref. [1])

$$\begin{aligned} \sigma(\nu_e n)_{\text{inelastic}} &= \sigma(\bar{\nu}_e p)_{\text{inelastic}} \\ &= 9.1 \times 10^{-42} \left(\frac{E_\nu}{10 \text{ MeV}} \right)^2 \text{ cm}^2, \\ \sigma(\nu n)_{\text{elastic}} &= 2.6 \times 10^{-42} \left(\frac{E_\nu}{10 \text{ MeV}} \right)^2 \text{ cm}^2, \\ &\quad (\text{all } \nu \text{ species}), \\ \sigma(\nu p)_{\text{elastic}} &= 2.1 \times 10^{-42} \left(\frac{E_\nu}{10 \text{ MeV}} \right)^2 \text{ cm}^2, \\ &\quad (\text{all } \nu \text{ species}). \end{aligned} \quad (2.2)$$

The total cross sections in the star medium for the species in question are then

$$\begin{aligned} \sigma_{\nu_e} &= Y_n [\sigma(\nu_e n)_{\text{inel.}} + \sigma(\nu n)_{\text{el.}}] + Y_p \sigma(\nu p)_{\text{el.}}, \\ \sigma_{\bar{\nu}_e} &= Y_p [\sigma(\bar{\nu}_e p)_{\text{inel.}} + \sigma(\nu p)_{\text{el.}}] + Y_n \sigma(\nu n)_{\text{el.}}, \\ \sigma_{\nu_x} &= Y_n \sigma(\nu n)_{\text{el.}} + Y_p \sigma(\nu p)_{\text{el.}}, \end{aligned} \quad (2.3)$$

which result in the hierarchy $\sigma_{\nu_e} > \sigma_{\bar{\nu}_e} > \sigma_{\nu_x}$. Consequently, the sizes of the respective neutrinospheres follow the same order and, since the star temperature is higher further inside, the average energies also follow a hierarchy [28]:

$$\begin{aligned} \langle E_{\nu_e} \rangle &\sim 10 \text{ MeV}, \quad \langle E_{\bar{\nu}_e} \rangle \sim 15 \text{ MeV}, \\ \langle E_{\nu_x} \rangle &\sim 20 \text{ MeV}. \end{aligned} \quad (2.4)$$

Concerning the neutrino spectra, we take two alternative approaches. In our first, simpler approach, we consider purely monoenergetic neutrinos for each species, as given in Eq. (II). Each species ν_i has then a definite neutrinosphere. In our second, more refined approach, we consider thermal (Fermi-Dirac) energy distributions for each neutrino species [29], with temperatures according to the energy averages given in Eq. (II). In this case, the neutrinospheres are continuously distributed.

We also checked for the possibility that neutrinos could experience flavor oscillations in matter while propagating

from the neutrinosphere towards the star surface, but found this effect to be irrelevant for the spin-down. Neutrino resonant conversion at energies near 10 MeV is important in the expanding envelope [30] where the matter density is $(10^{26} - 10^{27}) \text{ cm}^{-3}$, but in our region of interest of the star densities are about 10^{35} cm^{-3} (see Ref. [1]), where flavor oscillations are suppressed. Oscillations can happen, but in a rather thin layer close to the neutron star surface, and so their effect on the spin-down is negligible.

Another group of flavor changing processes, which can influence the angular momentum transfer by neutrinos, is the neutrino flavor conversion due to the $\nu - \nu$ scattering [31, 32]. This effect was shown to significantly change the initial flavor content of neutrinos in a dense neutrino flux, corresponding to the neutrino luminosity $\mathcal{L}_\nu > 10^{51} \text{ erg/s}$. It was however found in Ref. [32] that the significant transition probability due to $\nu - \nu$ collisions is archived at the distances (70 – 80) km from the neutrinosphere surface, i.e. it happens in the envelope of a star. On the contrary, we study the spin-down of PNS due to the collisions with background matter in the core of PNS outside the neutrinosphere at the distances $< 20 \text{ km}$ from the star center (see Fig. 2 below).

Note that background matter can also influence the collective neutrino flavor transformations. In order to have some resonance effects in these flavor changing processes, the neutrino density $n_\nu(r) = \mathcal{L}_\nu / 4\pi r^2 \langle E_\nu \rangle$, where $\langle E_\nu \rangle \sim 10 \text{ MeV}$ is the typical neutrino energy and $\mathcal{L}_\nu \sim 10^{52} \text{ erg/s}$, should be comparable with the electrons number density n_e . In our calculations we suggest that $n_e \approx 0.1 n_n \sim 10^{34} \text{ cm}^{-3}$ inside the core of PNS at $r < (15 - 20) \text{ km}$. The number density of neutrinos at the same distance is $n_\nu \sim 10^{32} \text{ cm}^{-3}$, which is 2 orders of magnitude less than the electron density. It means that the background matter is unlikely to generate any resonance effects in our case.

Now we should address the density profile of the star. The actual density profile strongly depends on the equation of state of the nuclear matter, so these density distributions are generally not well known [33]. Results of numerical simulations for the density profiles [34] can be approximated by the following expression:

$$n(r) = n_c \left(1 - \frac{r^2}{R^2} \right) \exp \left(-\epsilon \frac{r^2}{R^2} \right), \quad (2.5)$$

where n_c is the central density and ϵ is a phenomenological parameter. The $\epsilon = 0$ case corresponds to the well known Tolman VII model [35]. An analogous expression for the density profile was used in the study of nonradial oscillations of a neutron star [36]. In Fig. 1(a) we show the behavior of the density for various values of the parameter ϵ . In order not to obscure the sensitivity of our results to different parts of the calculation, yet with the risk of not being realistic in specific cases, we will use these analytical density profiles instead of full numerical profiles. As shown in Fig. 1(a), negative ϵ implies a more flat profile with a fast drop at the surface, while positive

values imply a gradual decrease of the density from the center to the surface.

From Eqs. (2.1), (2.3) and (2.5) we can get the radii of the neutrinospheres as functions of the parameter ϵ , for a given neutrino energy. In our analysis we use the values $n_c = (4.7 - 6.6) \times 10^{38} \text{ cm}^{-3}$ and $R = 15 \text{ km}$ as well as $n_c = (2.0 - 2.7) \times 10^{38} \text{ cm}^{-3}$ and $R = 20 \text{ km}$ for the central density and the star radius. The total mass of the star calculated on the basis of Eq. (2.5) has the form,

$$M \approx M_\odot \left(\frac{n_c}{10^{38} \text{ cm}^{-3}} \right) \left(\frac{R}{10 \text{ km}} \right)^3 F_M(\epsilon),$$

$$F_M(\epsilon) = \int_0^1 dx x^2 (1 - x^2) e^{-\epsilon x^2}. \quad (2.6)$$

For the chosen densities and radii Eq. (2.6) gives one the mass of PNS in the range $(1.4 - 2.0) M_\odot$, depending on the parameter ϵ . Although the mass of a neutron star strongly depends on the equation of state of the neutron star matter, it is unlikely bigger than $2 M_\odot$ [37]. In Fig. 1(b) we present the ϵ dependence of the function $F_M(\epsilon)$, which is proportional to the PNS mass.

Now, let us address the issue of emission directions. From the neutrinosphere, neutrinos are emitted outwards in all directions. However, as a simplified model for the spin-down effect, we approximate the emission as purely radial, where “radial” is meant in the frame comoving with the local matter at the neutrino production point. In reality, of course, neutrinos are produced in all directions and rigorously one should consider the whole hemisphere of outgoing directions at every point. However, those particles emitted more towards the tangential velocity will transfer less momentum to the star under subsequent scattering, while those emitted against the tangential velocity should transfer more momentum. In order to test the validity of the radial emission model, we performed the calculations in the case of neutrinos emitted in all directions within the equatorial plane and checked that indeed collisions with purely radially emitted neutrinos represent the full spin-down effect up to a geometrical factor near unity. Since there is no need for precision higher than a few tens of a percent, in what follows we will present the estimates within the model of radially produced neutrinos.

The process is then calculated by considering that neutrinos are emitted from their corresponding neutrinosphere and subsequently collide with the star medium on their way out, thus taking away part of the angular momentum.

Now let us describe the subsequent elastic collision of the outgoing neutrino with the star matter, which is where the spin down effect takes place. The effective weak interaction for elastic neutrino scattering with a

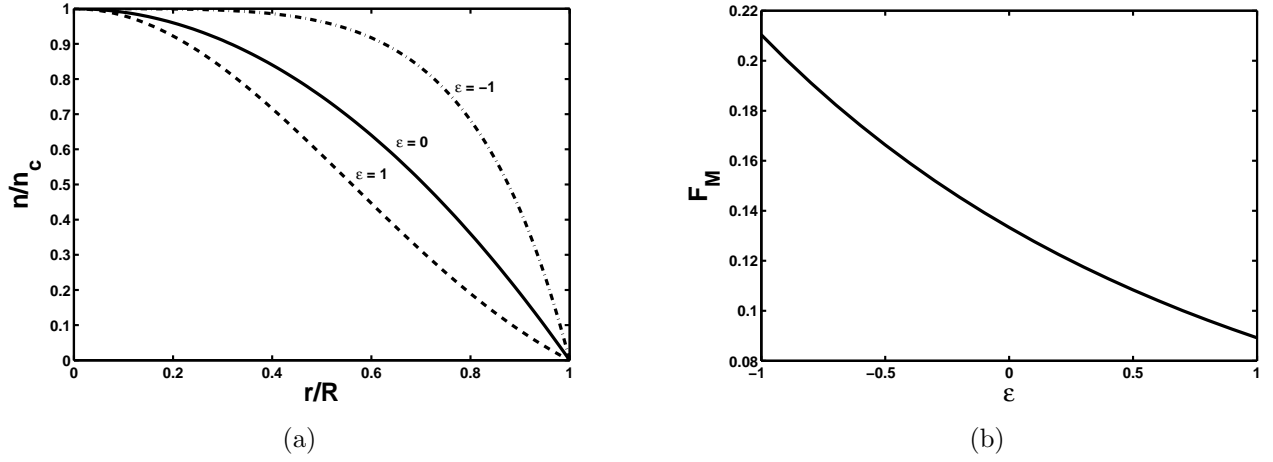


FIG. 1. (a) The radial dependence of the density for various values of the parameter ϵ . The solid line corresponds to the Tolman VII model ($\epsilon = 0$), the dashed line is built for $\epsilon = 1$, and the dash-dotted for $\epsilon = -1$. (b) The function $F_M(\epsilon)$, given in Eq. (2.6), which defines the star mass dependence on the density profile parameter ϵ .

TABLE I. The values of the coefficients $g_{L,R}$ in Eq. (2.7) for various channels of neutrino elastic scattering. ν_x stands for $x \neq e$ while ν stands for all lepton flavors.

No.	Reactions	g_L	g_R
1	$\nu_e e \rightarrow \nu_e e$	0.73	0.23
2	$\nu_x e \rightarrow \nu_x e$	-0.27	0.23
3	$\bar{\nu}_e e \rightarrow \bar{\nu}_e e$	0.23	0.73
4	$\bar{\nu}_x e \rightarrow \bar{\nu}_x e$	0.23	-0.27
5	$\nu p \rightarrow \nu p$	0.27	-0.23
6	$\nu n \rightarrow \nu n$	-0.50	0.00
7	$\bar{\nu} p \rightarrow \bar{\nu} p$	-0.23	0.27
8	$\bar{\nu} n \rightarrow \bar{\nu} n$	0.00	-0.50

background fermion f has the form [38],

$$M = \frac{G_F}{\sqrt{2}} \bar{f}(p_2) [g_L \gamma_\mu (1 - \gamma^5) + g_R \gamma_\mu (1 + \gamma^5)] f(p_1) \times \bar{\nu}(k_2) \gamma^\mu (1 - \gamma^5) \nu(k_1), \quad (2.7)$$

where $\nu(k_{1,2})$ are the initial and final neutrino spinors with momenta $k_{1,2} = (\omega_{1,2}, \mathbf{k}_{1,2})$, and $f(p_{1,2})$ are the respective spinors of the fermions in the medium, with momenta $p_{1,2} = (E_{1,2}, \mathbf{p}_{1,2})$ respectively. The coefficients $g_{L,R}$ depend on the neutrino scattering channel and are listed in Table I.

From the effective interaction of Eq. (2.7), we can build the cross section,

$$d\sigma(\nu f \rightarrow \nu f) = \frac{1}{64\pi^2} \delta^4(p_2 + k_2 - p_1 - k_1) \times \frac{|M|^2}{(k_1 \cdot p_1) \omega_2 E_2} d^3\mathbf{k}_2 d^3\mathbf{p}_2, \quad (2.8)$$

where the matrix element squared for unpolarized scat-

tering derived from Eq. (2.7) is

$$|M|^2 = 128 G_F^2 [g_L^2 (p_1 \cdot k_1)^2 + g_R^2 (p_1 \cdot k_2)^2 - g_L g_R m_f^2 (k_1 \cdot k_2)], \quad (2.9)$$

with m_f being the mass of the fermion f . For radially emitted neutrinos, and taking this radial direction at each collision point as our reference, the incoming fermion from the medium will be perpendicular and the outgoing neutrino will have an arbitrary direction parametrized by the relative polar and azimuthal angles θ_2 and ϕ_2 , such that

$$\mathbf{k}_1 = \omega_1(0, 0, 1), \quad \mathbf{p}_1 = E_1 v_f(0, 1, 0), \\ \mathbf{k}_2 = \omega_2(\sin \theta_2 \cos \phi_2, \sin \theta_2 \sin \phi_2, \cos \theta_2). \quad (2.10)$$

Here v_f is the tangential velocity of the star at the interaction point. We are assuming that the thermal velocities of the fermions in the medium average out concerning this effect, and the only effective velocity is the average drift of the medium due to rotation. With these conventions, the dot products of interest are

$$(p_1 \cdot k_1) = E_1 \omega_1, \quad (k_1 \cdot k_2) = \omega_1 \omega_2 (1 - \cos \theta_2), \\ (p_1 \cdot k_2) = E_1 \omega_2 (1 - v_f \sin \theta_2 \sin \phi_2). \quad (2.11)$$

We can integrate Eq. (2.8) over \mathbf{p}_2 to get the differential cross section,

$$\frac{d\sigma}{d\Omega_2} = \frac{|M|^2}{64\pi^2} \frac{\omega_2^2}{\omega_1^2 E_1^2}, \quad (2.12)$$

where the energy of the outgoing neutrino is given, by energy-momentum conservation, in terms of the scattering angles

$$\omega_2 = \frac{E_1 \omega_1}{E_1 (1 - v_f \sin \theta_2 \sin \phi_2) + \omega_1 (1 - \cos \theta_2)}. \quad (2.13)$$

Now we can calculate the rate of transverse momentum transferred to the star at that collision point. Let $J(r)$ be the (radial) neutrino flux incoming to a given collision point; then $J(r)(d\sigma/d\Omega_2)d\Omega_2$ is the rate of outgoing neutrinos within $d\Omega_2$. Since the \mathbf{e}_ϕ component of momentum of each of these outgoing neutrinos is $\omega_2 \sin \theta_2 \sin \phi_2$, then the total \mathbf{e}_ϕ momentum per unit time transferred to the star due to the outgoing neutrinos ejected from a given collision point is

$$\langle \dot{k}_\phi \rangle = \int \omega_2 \sin \theta_2 \sin \phi_2 J(r) \frac{d\sigma}{d\Omega_2} d\Omega_2, \quad (2.14)$$

where $d\Omega_2 = \sin \theta_2 d\theta_2 d\phi_2$. The flux $J(r)$ at the collision point is related to the neutrino flux at the surface of the star, J_0 , by the relation $J(r) = J_0 \times (R/r)^2$, where R is the star radius. Using Eq. (2.14) we can now calculate the total rate of angular momentum transferred to the star as a whole by just summing over all collision points that lie outside the corresponding neutrinosphere,

$$\dot{L}_z = \int_{r>R_{ns}} \langle \dot{k}_\phi \rangle r \sin \vartheta n_f(\mathbf{r}) d^3\mathbf{r}, \quad (2.15)$$

where $n_f(\mathbf{r})$ is the local number density of target fermions in the medium, and ϑ is the polar angle (colatitude) of the star at the collision point. The full result for \dot{L}_z is the sum of this type of calculation, repeated for each neutrino species.

The rate of angular momentum transfer to the star as given in Eq. (2.15) requires the computation of a four-fold integral which has to be evaluated numerically. Nevertheless, within the following approximations one can calculate an analytical expression for \dot{L}_z . First, assuming a star radius $R = 20$ km and angular velocity $\Omega = 10^3 \text{ s}^{-1}$, its equatorial linear velocity (in units of c) is ~ 0.1 . Thus we can treat v_f in Eq. (2.13) as a small parameter. In addition, typical energies for the emitted neutrinos are $\omega_1 \sim 10$ MeV, while the incoming fermion in the medium, which is nonrelativistic, has an energy E_1 near the nucleon mass. Therefore the ratio ω_1/E_1 is also small. Consequently, we use the approximation,

$$\omega_2 \approx \omega_1(1 + \xi), \quad (2.16)$$

where

$$\xi = v_f \sin \theta_2 \sin \phi_2 - \frac{\omega_1}{E_1}(1 - \cos \theta_2) \ll 1.$$

For the matter velocity at the collision point we use

$$v_f = v_0 \sin \vartheta \frac{r - R_{ns}}{R}, \quad (2.17)$$

where v_0 is the equatorial velocity of the neutron star. Here v_f corresponds to the *relative* transverse velocity of the medium at the collision point (radius r) with respect to the velocity of the medium at the neutrino emission point (radius R_{ns}).

Using Eq. (2.9) and Table I, we can determine the square of the matrix element, for example for the specific reaction $\nu_e n \rightarrow \nu_e n$, which is $|M|^2 = 32G_F^2 E_1^2 \omega_1^2$. Consequently, using Eqs. (2.15) and (2.16) one gets the following approximation for the rate \dot{L}_z due to this type of collision:

$$\begin{aligned} \dot{L}_z &\approx 2G_F^2 \omega_1^3 R J_0 v_0 \int_{R_{ns}}^R r(r - R_{ns}) dr \\ &\times \int_0^\pi n_n(r, \vartheta) \sin^3 \vartheta d\vartheta, \end{aligned} \quad (2.18)$$

where $n_n(r, \vartheta)$ is the neutron density at the corresponding collision point.

It is convenient to present the final result as the ratio between the rate of angular momentum loss and the initial angular momentum of the star $L_0 = \mathcal{I} \Omega$, where its moment of inertia is given by

$$\mathcal{I} = \frac{8\pi}{3} m_n \int_0^R dr r^4 n(r), \quad (2.19)$$

and where m_n is the neutron mass. Based on Eqs. (2.5) and (2.18) we find for this ratio:

$$\begin{aligned} \frac{\dot{L}_z}{L_0} &= \frac{G_F^2 \mathcal{L}_\nu E_\nu^2}{4\pi^2 R^2 m_n} \frac{F_1(\epsilon)}{F_0(\epsilon)} \\ &\approx 1.0 \text{ s}^{-1} \times \left(\frac{E_\nu}{10 \text{ MeV}} \right)^2 \left(\frac{\mathcal{L}_\nu}{10^{52} \text{ erg/s}} \right) \\ &\times \left(\frac{R}{10 \text{ km}} \right)^{-2} \frac{F_1(\epsilon)}{F_0(\epsilon)}, \end{aligned} \quad (2.20)$$

where \mathcal{L}_ν is the neutrino luminosity and where we have defined the following integrals:

$$\begin{aligned} F_0(\epsilon) &= \int_0^1 dx x^4 (1 - x^2) e^{-\epsilon x^2}, \\ F_1(\epsilon) &= \int_{x_0}^1 dx x(x - x_0)(1 - x^2) e^{-\epsilon x^2}, \end{aligned} \quad (2.21)$$

with $x_0 \equiv R_{ns}/R$.

We have just considered the reaction $\nu_e n \rightarrow \nu_e n$. The contributions of all other neutrino species, including collisions with protons, are treated in a similar way and added to the result. The average neutrino luminosity just after the neutronization stage [28] is $\mathcal{L}_\nu \sim 10^{52} \text{ erg/s}$. This large neutrino luminosity lasts for a few seconds, mainly during the Kelvin-Helmholtz stage, with all neutrino types, $\nu_{e,\mu,\tau}$ and $\bar{\nu}_{e,\mu,\tau}$, having almost equal luminosities, and therefore giving similar contributions to Eq. (2.20).

A refinement of this neutrino emission model considers the three neutrino species not monoenergetic but with thermal distributions, each with distinct temperatures and chemical potentials. Therefore we can choose the

Fermi-Dirac distribution in the form [29]

$$\frac{dN}{dE_\nu} = \frac{\mathcal{L}_\nu}{F(\eta_\nu)T_\nu^4} \frac{E_\nu^2}{\exp(E_\nu/T_\nu - \eta_\nu) + 1},$$

$$F(\eta_\nu) = \int_0^\infty dx \frac{x^3}{e^{x-\eta_\nu} + 1}, \quad (2.22)$$

where we have the relation $\langle E_\nu \rangle / T_\nu \approx 3.1514 + 0.1250\eta_\nu + 0.0429\eta_\nu^2 + \dots$ between the temperature of the neutrino gas T_ν and the mean neutrino energy $\langle E_\nu \rangle$ defined in Eq. (II). The typical values of the chemical potentials are (see Ref. [29]) $\eta_{\nu_e} \approx 2$, $\eta_{\bar{\nu}_e} \approx 3$, and $\eta_{\nu_x} \approx 1$.

On the basis of Eqs. (2.20)-(2.22) we get the averaged ratio as

$$\left\langle \frac{\dot{L}_z}{L_0} \right\rangle \approx 1.0 \text{ s}^{-1} \times \left(\frac{T_\nu}{10 \text{ MeV}} \right)^{-4}$$

$$\times \left(\frac{\mathcal{L}_\nu}{10^{52} \text{ erg/s}} \right) \left(\frac{R}{10 \text{ km}} \right)^{-2}$$

$$\times \frac{1}{F(\eta_\nu)} \int_0^\infty \frac{y^5 dy}{e^{y-\eta_\nu} + 1} \frac{F_1(\epsilon, y)}{F_0(\epsilon)}, \quad (2.23)$$

where we are including the energy dependence of the function $F_1(\epsilon)$ in Eq. (2.21) in the form of the dimensionless parameter $y = (E_\nu/10 \text{ MeV})$, since the size of the neutrinosphere depends on the neutrino energy [see Eqs. (2.1) and (2.2)].

In Fig. 2 we present the total angular momentum carried away by all neutrino species, $L_z = \sum_i \dot{L}_z(\nu_i) \Delta t$, where $\Delta t = 10 \text{ s}$, in units of the initial angular momentum L_0 , versus the mass of PNS. Here Δt is the time interval during which the luminosity stays at the high value $\mathcal{L}_\nu \approx 10^{52} \text{ erg/s}$. Note that the PNS mass variation on this plot results from its epsilon dependence [see Eq. (2.6) and Fig. 1(b)].

As one can see from the figures, a larger fraction of the angular momentum can be carried away by neutrinos for a star with bigger radius. We can also notice that with the enhancement of the central density the effect increases. On one hand, the neutrinosphere radius grows with the enhancement of the central density (2.1). Thus neutrinos have less opportunity to collide with rotating matter and the relative velocities from production to collision are also smaller. On the other hand, PNS with equal masses and different central densities correspond to a different ϵ parameter in Eq. (2.6). For example, $n_c = 4.7 \times 10^{38} \text{ cm}^{-3}$ corresponds to $\epsilon = 1$ and $n_c = 6.6 \times 10^{38} \text{ cm}^{-3}$ to $\epsilon = 2$ for $M = 1.4M_\odot$. The bigger value of ϵ implies a more steep density profile near the central region and, hence, a bigger concentration of PNS mass there. It means that effectively a neutrinosphere should decrease at higher ϵ . The results of numerical simulations presented in Fig. 2 shows that the latter effect is more significant.

One can also see in Fig. 2 that the difference between the models of monoenergetic and thermally distributed

neutrinos is less than several percent. Thus, a monoenergetic neutrino model is still a good approximation to describe the spin-down.

Including general relativity corrections to the moment of inertia of the neutron star, the values of \dot{L}_z/L_0 become slightly smaller than those we obtained. For example, if we consider a neutron star with $M = 2M_\odot$, the reduction factors within the Tolman VII model ($\epsilon = 0$) will be ≈ 0.76 for $R = 15 \text{ km}$ and ≈ 0.82 for $R = 20 \text{ km}$ [34]. As a result, we find that, by the mechanism we have considered, and within the Tolman VII model as benchmark ($\epsilon = 0$) for a $R = 15 \text{ km}$ star, neutrinos could carry away up to 2.4×10^{-4} of the initial angular momentum of the PNS [compare this value to the corresponding result shown in Fig. 1(a), which does not include the general relativity corrections].

For other density profiles, i.e., corresponding to $M = 1.4M_\odot$ ($\epsilon = 2$), neutrinos can carry away 1.7×10^{-3} of the initial angular momentum for a star with $R = 20 \text{ km}$ and $n_c = 2.8 \times 10^{38} \text{ cm}^{-3}$. This result is significantly less than predicted in the previous works [12, 13].

What follows at later stages of the neutron star evolution is that the neutrinospheres shrink as the star cools down, because the mean free path grows beyond the star radius. This is mainly due to the Pauli blocking reduction of the neutrino scattering cross section. At the same time, the neutrino flux drops down dramatically from its initial values. The expression in Eq. (2.20) is then valid only at the initial stages, which is the only time when the spin-down due to neutrino emission can be of any significance.

III. SUMMARY AND CONCLUSIONS

We have studied the spin-down of a forming neutron star due to neutrino emission. The spin-down by neutrino emission is significant only for the first few seconds of the neutron star evolution, when the size of the neutrinosphere is less than (but comparable to) the radius of the star and the neutrino flux is still large. These conditions allow for neutrinos to have a large enough collision rate. At later stages the star becomes almost transparent for neutrinos and the neutrino flux is too small for this effect to be of any significance, so other spin-down mechanisms take over.

We model the phenomenon by considering neutrinos of type ν_e , $\bar{\nu}_e$, and ν_x (where x stands for all other), which have different interaction with the medium, each produced at their corresponding neutrinosphere and moving radially outwards, subsequently colliding with the star matter in the outer shells, where the transverse velocity of the medium is larger than at the production point, thus causing a slowing down of the star.

An arguable part of the model is the consideration of purely radially moving neutrinos at the production points, but we have checked analytically in some simplified cases that the emission in all directions causes an

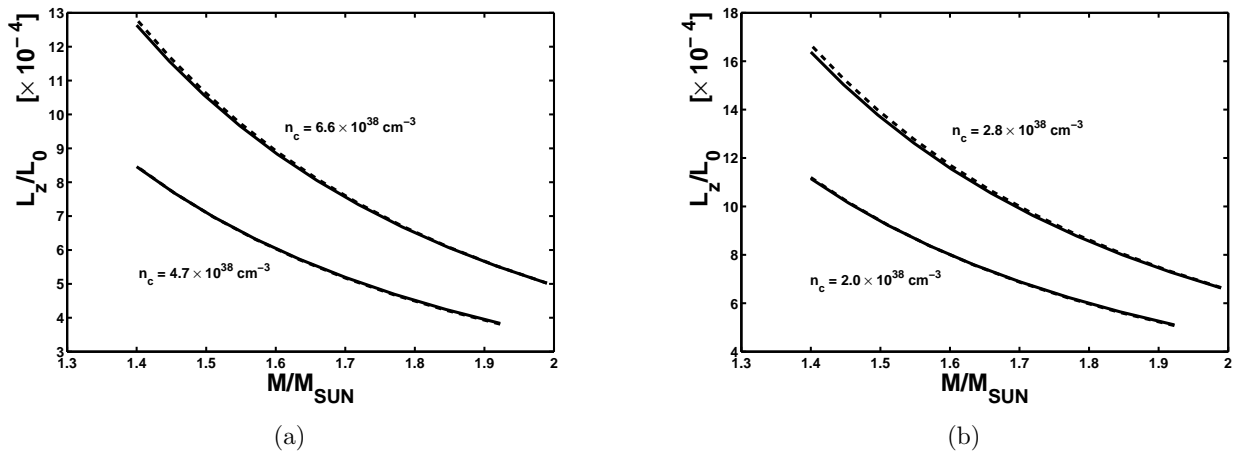


FIG. 2. The fraction of the total angular momentum carried away by all neutrinos types versus the PNS mass, which depends on the parameter ϵ according to Eq. (2.6), for various central densities. The dashed lines correspond to the simple model (2.20) with monoenergetic neutrinos with energies given in Eq. (II). The solid lines correspond to the refined model (2.23) with thermally distributed neutrinos with average energies (temperatures) given in Eq. (II). (a) The fraction for a star with $R = 15$ km. The upper curves correspond to $n_c = 6.6 \times 10^{38} \text{ cm}^{-3}$ and the lower ones to $n_c = 4.7 \times 10^{38} \text{ cm}^{-3}$. (b) The fraction for a star with $R = 20$ km. The upper curves correspond to $n_c = 2.7 \times 10^{38} \text{ cm}^{-3}$ and the lower ones to $n_c = 2.0 \times 10^{38} \text{ cm}^{-3}$.

average effect not much different than the purely radial case.

Another simplification is that Pauli blocking and other nucleon correlations are not taken into account, presuming that they are more important at later stages, when neutrino flux and energies are lower and this spin-down mechanism is negligible.

Another important part of the model concerns the density profile, where we use a phenomenological analytical expression instead of more realistic numerical profiles, in order to study the sensitivity to it and have a better comparison to previous estimates to the spin-down phenomenon. We find that the density distribution, $n(r)$, significantly affects the results for the rate of angular momentum loss (see Fig. 1). Very few analytical formulas for $n(r)$ models are known, and the majority of the density profiles are available from numerical simulations. We have chosen an exponential density profile (2.5) which depends on a phenomenological parameter ϵ to fit the results of the numerical simulations [34]. For $\epsilon = 0$ this formulation reproduces the well known Tolman VII model. Although this model cannot capture the fine details of individual cases, it reproduces the main features of realistic stars. However, it is unable to explain without fine tuning the enormous range of matter densities, from $\sim 10^6 \text{ g/cm}^3$ in the crust to $> 10^{14} \text{ g/cm}^3$ in the center. Therefore we have introduced an additional exponential factor in the model for $n(r)$.

As shown in Fig. 1(a), for positive ϵ the density goes gradually down, while for negative ϵ it stays high almost all over the star, falling sharply at the surface. Consistently, Fig. 2 shows that the spin-down effect is bigger for PNS with smaller mass at the fixed central density. Taking into account Fig. 1(b) we obtain that spin-down should increase with the enhancement of ϵ because a

higher and flatter density implies a larger neutrinosphere radius, thus decreasing the relative velocity of the star at the collision point with respect to the point of production. On the contrary, if neutron stars would feature a more gradual density descent, the average distance from the neutrinospheres to the collision points will increase, causing a stronger spin-down effect.

We have found that, for some density profiles corresponding to $\epsilon = 2$ in the case of a PNS with $R = 20$ km and central density $n_c = 2.8 \times 10^{38} \text{ cm}^{-3}$, which gives one $M = 1.4 M_\odot$, neutrinos can carry away up to about 1.7×10^{-3} of the initial angular momentum of the neutron star, provided that an average neutrino luminosity near $\mathcal{L}_\nu = 10^{52} \text{ erg/s}$ lasts for about 10 s during the Kelvin-Helmholtz stage of the neutron star evolution. The results of our calculations for other central densities and radii are presented in Fig. 2.

We should recall that previous estimates [12, 13] gave larger values of \dot{L}_z , and it was even predicted that the rotation of a neutron star could be stopped by neutrino emission (or equivalently, a reduction of the angular velocity by more than an order of magnitude). After using a variable density profile, our better knowledge of electroweak interactions today, and the most recent data on the neutrino flux, we find that the results are clearly not as dramatic.

Let us examine the importance of various factors which were not accounted for in the previous calculations of the PNS spin down [12, 13]. For example, we can discuss the situation when all neutrinos are monoenergetic, with $E_\nu \sim 10 \text{ MeV}$ and $\mathcal{L}_\nu \sim 10^{52} \text{ erg/s}$, and are emitted from the PNS center, whereas the density profile is given by Eq. (2.5). The considered case is equivalent to the neutrinosphere with zero radius: $x_0 = 0$ in Eq. (2.21). Using Eq. (2.20) for PNS with $R \sim (15 - 20) \text{ km}$, we obtain that

$\dot{L}_z \Delta t \sim L_0$, where $\Delta t \sim$ several seconds. Therefore we obtain that the rotation of PNS can be significantly reduced by the neutrino emission provided all the particles are emitted in the center of PNS, which reproduces the results of Refs. [12, 13]. It means that the concept of the neutrinosphere is the most important in our calculations.

It can be also shown that various density distribution profiles can change the PNS spin-down, however not so dramatically. Concerning other corrections, the inclusion of Pauli blocking or nucleon correlations would tend to make the effect even smaller; different proportions of neutrino species or neutrino oscillations only induce minor or negligible changes; using monoenergetic or thermally distributed neutrinos also result in minor differences in the spin-down effect.

Concerning the experimental observation of this effect,

unfortunately there is quite limited information about the initial angular velocities of neutron stars. An effort to infer initial angular velocities of PNS has been made [39], where it was revealed that there should be a large uncertainty in the results.

ACKNOWLEDGMENTS

This work has been supported by Fondecyt (Chile) Grant No. 1070227 and Conicyt (Chile), Programa Bicentenario PSD-91-2006. We also thank L. B. Leinson, J. Maalampi, G. G. Raffelt, A. Reisenegger, I. Schmidt and A. I. Studenikin for helpful discussions. One of the authors (MD) is grateful to Deutscher Akademischer Austausch Dienst for a grant. The comments of the referee are also appreciated.

-
- [1] C. Giunti and C. W. Kim, *Fundamentals of neutrino physics and astrophysics* (Oxford University Press, New York, 2007), pp. 511–528.
 - [2] K. S. Hirata, *et al.*, Phys. Rev. Lett. **58**, 1490 (1987); Phys. Rev. D **38**, 448 (1988).
 - [3] R. M. Bionta, *et al.*, Phys. Rev. Lett. **58**, 1494 (1987); C. B. Bratton, *et al.*, Phys. Rev. D **37**, 3361 (1988).
 - [4] E. N. Alekseev *et al.*, JETP Lett. **45**, 589 (1987); Phys. Lett. B **205**, 209 (1988); A. E. Chudakov, *et al.*, JETP Lett. **46**, 373 (1987).
 - [5] V. L. Dadykin, *et al.*, JETP Lett. **45**, 593 (1987); M. Aglietta, *et al.*, Europhys. Lett. **3**, 1315 (1987).
 - [6] J. M. Lattimer, C. J. Pethick, M. Prakash, P. Haensel, Phys. Rev. Lett. **66**, 2701 (1991); J. M. Lattimer and M. Prakash, Science **304**, 536 (2004).
 - [7] D. G. Yakovlev and C. J. Pethick, Ann. Rev. Astron. Astroph., **42**, 169 (2004), astro-ph/0402143.
 - [8] J. N. Bahcall, M. H. Pinsonneault, and S. Basu, Astrophys. J. **555**, 990 (2001), astro-ph/0010346; J. N. Bahcall and M. H. Pinsonneault, Phys. Rev. Lett. **92**, 121301 (2004), astro-ph/0402114.
 - [9] M. Liebendörfer, A. Mezzacappa, O. Messer, G. Martinez, W. Hix, and F-K. Thielemann, Nucl. Phys. A **719**, 144 (2003), astro-ph/0211329.
 - [10] A. Kusenko and G. Segre, Phys. Rev. Lett. **77**, 4872 (1996), hep-ph/9606428; Phys. Rev. D **59**, 061302 (1999), astro-ph/9811144.
 - [11] E. Kh. Akhmedov, A. Lanza, and D. W. Sciama, Phys. Rev. D **56**, 6117 (1997), hep-ph/9702436; D. Grasso, H. Nunokawa, and J. W. F. Valle, Phys. Rev. Lett. **81**, 2412 (1998), astro-ph/9803002; H.-T. Janka and G. G. Raffelt, Phys. Rev. D **59**, 023005 (1999), astro-ph/9808099; P. Arras and D. Lai, Phys. Rev. D **60**, 043001 (1999), astro-ph/9811371; Astrophys. J. **519** 745 (1999).
 - [12] K. O. Mikaelian, Astrophys. J. **214**, L22 (1977).
 - [13] R. Epstein, Astrophys. J. **219**, L39 (1978).
 - [14] F. Pacini, Nature **216**, 567 (1967); J. E. Gunn and J. P. Ostriker, Nature **221**, 454 (1969); Astrophys. J. **157**, 1395 (1969); R. N. Manchester and J. H. Taylor, *Pulsars*, (Freeman, San Francisco, California, 1977); P. Goldreich and W. Julian, Astrophys. J. **157**, 869 (1969); I. Contopoulos and A. Spitkovsky, Astrophys. J. **643**, 1139 (2006), astro-ph/0512002; see also D. R. Lorimer and M. Kramer, *Handbook of Pulsar Astronomy* (Cambridge University Press, Cambridge, UK, 2005).
 - [15] G. G. Raffelt, *Stars as Laboratories for Fundamental Physics: the Astrophysics of Neutrinos, Axions, and other Weakly Interacting Particles* (Chicago Univ. Press, Chicago, 1996), pp. 395–448.
 - [16] A. A. Gvozdev and I. S. Ognev, JETP **94**, 1043 (2002), astro-ph/0403011.
 - [17] R. Epstein, Astrophys. J. **223**, 1037 (1978).
 - [18] T. W. Baumgarte and S. L. Shapiro, Astrophys. J. **504**, 431 (1998), astro-ph/9801294.
 - [19] H.-T. Janka, in *IAU Symposium 218, Young Neutron Stars and Their Environments*, ed. by F. Camilo and B. M. Gaensler (San Francisco, ASP, 2004), p. 3, astro-ph/0402200.
 - [20] T. A. Thompson, E. Quataert, and A. Burrows, Astrophys. J. **620**, 861 (2005), astro-ph/0403224.
 - [21] S. Akiyama and J. C. Wheeler, Astrophys. J. **629**, 414 (2005), astro-ph/0504563.
 - [22] T. A. Thompson, P. Chang, and E. Quataert, Astrophys. J. **611**, 380 (2004), astro-ph/0401555.
 - [23] A. Heger, S. E. Woosley, and H. C. Spruit, Astrophys. J. **626**, 350 (2005), astro-ph/0409422.
 - [24] C. D. Ott, A. Burrows, T. A. Thompson, E. Livne, and R. Walder, Astrophys. J. Suppl. Ser. **164**, 130 (2006), astro-ph/0508462.
 - [25] O. F. Dorofeev, V. N. Rodionov, and I. M. Ternov, JETP Lett. **40**, 917 (1984).
 - [26] A. Mezzacappa, M. Liebendörfer, C. Y. Cardall, O. E. B. Messer, and S. W. Bruenn, in *Stellar Collapse*, ed. by C. L. Fryer (Kluwer, Dordrecht, 2004), p. 101.
 - [27] S. Reddy, M. Prakash, J. M. Lattimer, and J. A. Pons, Phys. Rev. C **59**, 2888 (1999), astro-ph/9811294.
 - [28] T. Totani, K. Sato, H. E. Dalhed, and J. R. Wilson, Astrophys. J. **496**, 216 (1998), astro-ph/9710203.
 - [29] M. Th. Keil, G. G. Raffelt, and H.-T. Janka, Astrophys. J. **590**, 971 (2003), astro-ph/0208035.

- [30] R. Tòmas, M Kachelrieß, G. Raffelt, A. Dighe, H.-T. Janka, L. Scheck, JCAP **0409**, 015 (2004), astro-ph/0407132.
- [31] D. Nötzold and G. Raffelt, Nucl. Phys. B **307**, 924 (1988); J. T. Pantaleone, Phys. Rev. D **46**, 510 (1992); G. Sigl and G. Raffelt, Nucl. Phys. B **406**, 423 (1993).
- [32] H. Duan, G. M. Fuller, and Y.-Z. Qian, Phys. Rev. D **74**, 123004 (2006), astro-ph/0511275; H. Duan, G. M. Fuller, J. Carlson, and Y.-Z. Qian, *ibid.* **74**, 105014 (2006), astro-ph/0606616; *ibid.* **75**, 125005 (2007), astro-ph/0703776.
- [33] P. S. Negi, Int. J. Theor. Phys. **45**, 1684 (2006); gr-qc/0401024.
- [34] J. M. Lattimer and M. Prakash, Astrophys. J. **550** 426 (2001); astro-ph/0002232.
- [35] R. C. Tolman, Phys. Rev. **55**, 364 (1939).
- [36] D. V. Podgainyi, S. I. Bastrukov, I. V. Molodtsova, and V. V. Papoyan, Astrophysics **39** 278 (1996).
- [37] P. Haensel, A. Y. Potekhin, and D. G. Yakovlev, *Neutron Stars 1: Equation of State and Structure* (Springer, NY, 2007), pp. 297–301.
- [38] L. B. Okun', *Leptons and Quarks* (Nauka, Moscow, 1990), 2nd ed., pp. 150–157.
- [39] E. van der Swaluw and Y. Wu, Astrophys. J. **555**, L49 (2001); astro-ph/0104390.